Contribution from the Département de Physique Générale, SCM URA CNRS 331, CEA—Centre d'Etudes Nucléaires de Saclay, 91191 Gif sur Yvette Cedex, France

Preparation, Characterization, and Crystal Structure of $[ClO_2]^+[RuF_6]^-$. Crystal Structure of $[ClF_2]^+[RuF_6]^-$

Roland Bougon,* Walter V. Cicha, Monique Lance, Laurent Meublat, Martine Nierlich, and Julien Vigner

Received March 20, 1990

Chloryl hexafluororuthenate(V), $[ClO_2]^+[RuF_6]^-$, is prepared either by fluorination of RuO_4 using ClF_3 in HF solution at room temperature or by the reaction of ClO_2F with RuF_5. This salt, which like its counterpart $[ClF_2]^+[RuF_6]^-$ is a powerful oxidizer, is characterized by elemental analysis, X-ray powder data, and vibrational spectroscopy. The crystal structure of this salt shows that the ruthenium atom, located on a C_2 axis, is surrounded by a weakly distorted octahedron of fluorine atoms with six comparable bond lengths. The space group, unit cell parameters, and R factor are as follows: monoclinic, $P2/n$ (No. 13), a = 7.187 (6) Å, b = 5.653 (3) Å, c = 7.260 (5) Å, β = 90.87 (6)°, V = 294.9 (6) Å^3, Z = 2, R = 0.055. The structure of difluorochlorine(III) hexafluororuthenate(V), $[ClF_2]^+[RuF_6]^-$, obtained from the reaction of an excess of ClF_3 with RuF_5, is also reported and its characteristics are compared with those of $[ClO_2]^+[RuF_6]^-$. The space group, unit cell parameters, and R factor of $[ClF_2]^+[RuF_6]^-$ are as follows: orthorhombic, *Pcca* (No. 54), a = 19.957 (4) Å, b = 5.649 (2) Å, c = 10.616 (6) Å, V = 1197 (1) Å^3, Z = 8, R = 0.038. The vibrational spectra of both salts are discussed in light of the structures determined.

Introduction

As part of an ongoing study in our laboratory of transition metals in very high oxidation states, the chemistry of ruthenium fluorides and oxyfluorides is of interest. These materials are also of some value to the nuclear industry.[1] One of the primary interests concerns the fluorination of ruthenium oxides by fluorinating agents of variable strength. It was recently shown[2] for instance that ruthenium tetraoxide, RuO_4, can be fluorinated by krypton difluoride, KrF_2, in HF solution to form ruthenium oxide tetrafluoride, $RuOF_4$. The present paper reports further studies dealing with the fluorination of RuO_4, namely the reaction of the oxide with chlorine trifluoride, ClF_3, to yield the novel salt $[ClO_2]^+[RuF_6]^-$. This salt extends the range of derivatives of ruthenium pentafluoride, the acidic properties of which have already been demonstrated through the formation of complexes with a range of fluoride ion donors.[3-9]

The only other characterized salt derivative of RuF_5 with a triatomic cation is $[ClF_2]^+[RuF_6]^-$. However, the presence of some puzzling anomalies in the vibrational spectra resulted in an incomplete discussion.[6] A safer preparative method and reinvestigation of the properties of this salt are therefore also reported here, together with its crystal structure.

The single-crystal X-ray structures of $[ClF_2]^+[RuF_6]^-$ and $[ClO_2]^+[RuF_6]^-$ presented here are of interest for a number of reasons. First, they are the first examples of salts that contain an oxidized halogen together with a transition-metal anion for which the structure has been determined. Interestingly, although there are a fair number of known $[ClF_2]^+$ derivatives[10] and an even larger number of salts containing the $[ClO_2]^+$ cation,[11-21] only $[ClF_2]^+[PtF_6]^-$,[15,22] $[ClO_2]^+[PtF_6]^-$,[15] and $[ClO_2]^+[IrF_6]^-$[15] involve fluoride anions with transition-metal centers. This may be due at least in part to the experimental difficulties associated with the preparation of these materials and to the high electron affinity of many neutral transition-metal fluorides that exist in high oxidation states.[23] The somewhat related salt $[ClO_2]^+[Ru(SO_3F)_4]^-$ has also been reported, but the results from its characterization were not discussed in detail.[17] Only two single-crystal X-ray structures are known with $[ClF_2]^+$ as the cation,[24,25] whereas $[ClO_2]^+$ fares slightly better with four known structures,[14,20,26,27] although none surprisingly involve a discrete

Table I. X-ray Powder Diffraction Data for $[ClO_2]^+[RuF_6]^-$ and $[ClF_2]^+[RuF_6]^-$

$[ClO_2]^+[RuF_6]^-$				$[ClF_2]^+[RuF_6]^-$			
d, Å				*d*, Å			
obsd	calcd	intens	*hkl*	obsd	calcd	intens	*hkl*
5.67	5.653	m	010	5.62	5.65	ms	010
5.12	5.146	m	100	5.30	5.31	m	002
	5.069		$\bar{1}02$				
4.42	4.443	w	011	5.13	5.130	w	102
3.80	3.805	vs	110	5.00	4.990	m	400
3.60	3.593	s	002	4.44	4.460	s	211
3.04	3.054	mw	$\bar{2}12$	3.88	3.868	s	012
	3.032		012				
2.82	2.826	mw	020	3.78	3.797	s	112
	2.824		$\bar{2}11$				
2.63	2.634	w	$\bar{1}21$	3.61	3.607	s	212
	2.630		021				
2.57	2.573	vw	200	3.05	3.057	vw	412
2.47	2.477	w	120	2.86	2.866	vw	610
2.29	2.304	mw	$\bar{3}02$	2.76	2.767	vw	611
	2.285		102				
2.22	2.221	ms	022	2.63	2.633	w	221
					2.631		104
2.12	2.129	m	121	2.22	2.227	mw	613
1.88	1.884	mw	030	2.10	2.110	mw	621
					2.096		812
				1.84	1.839	w	623
				1.82	1.823	w	231

(1) Bourgeois, M.; Cochet-Muchy, B. Commissariat à l'Energie Atomique, 1971; BIST No. 161, p 41.
(2) Meublat, L.; Lance, M.; Bougon, R. *Can. J. Chem.* **1989**, *67*, 1729.
(3) Sladky, F. O.; Bulliner, P. A.; Bartlett, N. *J. Chem. Soc. A* **1969**, 2179.
(4) Prusakov, V. N.; Sokolov, V. B.; Chaivanov, B. B. *J. Appl. Spectrosc. (Engl. Transl.)* **1972**, *17*, 920.
(5) Griffiths, J. E.; Sunder, W. A.; Falconer, W. E. *Spectrochim. Acta* **1975**, *31A*, 1207.
(6) Burns, R. C.; O'Donnell, T. A. *J. Inorg. Nucl. Chem.* **1980**, *42*, 1613.
(7) Selig, H.; Sunder, W. A.; Disalvo, F. A.; Falconer, W. E. *J. Fluorine Chem.* **1978**, *11*, 39.
(8) Sunder, W. A.; Wayda, A. L.; Distefano, D.; Falconer, W. E.; Griffiths, J. E. *J. Fluorine Chem.* **1979**, *14*, 299.
(9) Bartlett, N.; Gennis, M.; Gibler, D. D.; Morrell, B. K.; Zalkin, A. *Inorg. Chem.* **1973**, *12*, 1717.
(10) Shamir, J. *Struct. Bonding* **1979**, *37*, 141 and references therein.
(11) Holloway, J. H.; Laycock, D. *Adv. Inorg. Chem. Radiochem.* **1983**, *27*, 157.
(12) Christe, K. O.; Schack, C. J.; Pilipovich, D.; Sawodny, W. *Inorg. Chem.* **1969**, *8*, 2489.
(13) Carter, H. A.; Aubke, F. *Can. J. Chem.* **1970**, *48*, 3456.
(14) Mallouk, T. E.; Desbat, B.; Bartlett, N. *Inorg. Chem.* **1984**, *23*, 3160.
(15) Christe, K. O. *Inorg. Chem.* **1973**, *12*, 1580.
(16) Woolf, A. A. *J. Chem. Soc.* **1954**, 4113.
(17) Leung, P. C.; Aubke, F. *Can. J. Chem.* **1984**, *62*, 2892.
(18) Yeats, P. A.; Aubke, F. *J. Fluorine Chem.* **1974**, *4*, 243.
(19) Carter, H. A.; Qureshi, A. M.; Aubke, F. *J. Chem. Soc., Chem. Commun.* **1968**, 1461.
(20) Edwards, A. J.; Sills, R. J. C. *J. Chem. Soc., Dalton Trans.* **1974**, 1726.
(21) Karelin, A. I.; Nikitina, Z. K.; Kharitonov, Y. Y.; Rosolovskii, V. Y. *Russ. J. Inorg. Chem. (Engl. Transl.)* **1970**, *15*, 480.
(22) (a) Bartlett, N.; Lohmann, D. H. *J. Chem. Soc.* **1964**, 619. (b) Grestsena, F. P.; Toeniskoetter, R. H. *Inorg. Chem.* **1966**, *5*, 1925.
(23) Bartlett, N. *Angew. Chem., Int. Ed. Engl.* **1968**, *7*, 433.
(24) Edwards, A. J.; Sills, R. J. C. *J. Chem. Soc. A* **1970**, 2697.
(25) Lynton, H.; Passmore, J. *Can. J. Chem.* **1971**, *49*, 2539.

0020-1669/91/1330-0102$02.50/0

Table II. Crystallographic Data for $[ClO_2]^+[RuF_6]^-$ and $[ClF_2]^+[RuF_6]^-$

	$[ClO_2]^+[RuF_6]^-$	$[ClF_2]^+[RuF_6]^-$
fw	282.51	288.51
space group	*P2/n*	*Pcca*
a, Å	7.187 (6)	19.957 (4)
b, Å	5.653 (3)	5.649 (2)
c, Å	7.260 (5)	10.616 (6)
β, deg	90.87 (6)	
V, Å^3	294.9 (6)	1197 (1)
Z	2	8
T, K	295	295
λ, Å	0.71073	0.71073
d(calcd), g cm^{-3}	3.181	3.202
μ, cm^{-1}	31.38	31.19
abs cor (min–max)	0.70–1.26	0.81–1.08
$R(F_o)$	0.055	0.038
$R_w(F_o)$	0.065	0.042

$[MF_6]^-$ type anion. Finally, the only previous structural reports[9] for $[RuF_6]^-$ are those of $[XeF]^+[RuF_6]^-$ and $[XeF_5]^+[RuF_6]^-$. One of the goals of this work was therefore to gain a deeper understanding of the nature of the interaction between $[RuF_6]^-$ (and by analogy other $[MF_6]^-$ type transition-metal anions) and cations capable of forming interionic contacts.

Experimental Section

Apparatus. Volatile fluorides were manipulated in a Monel Teflon-FEP vacuum manifold. Prior to handling of the moisture-sensitive compounds, the system was passivated with ClF_3 or hot fluorine. The synthesis was achieved in Monel vessels or in Teflon-FEP or sapphire tubes equipped with Monel or Teflon-FEP valves. Moisture-sensitive nonvolatile materials were handled in the dry nitrogen atmosphere of a glovebox. Infrared spectra were recorded in the range 4000–200 cm^{-1} on a Perkin-Elmer Model 283 spectrophotometer. Spectra of solids were obtained by using dry powders pressed between AgBr or AgCl windows in an Econo press (Barnes Engineering Co.). Raman spectra were recorded on a Coderg Model T800 spectrophotometer using the 514.5-nm excitation line of an Ar ion Model 165 Spectra-Physics laser filtered with a Coderg premonochromator. Solutions were examined in a Teflon-FEP or sapphire tube. In the range of observation, the frequency accuracy was estimated to be approximately ±3 cm^{-1} for the infrared spectra and ±1 cm^{-1} for the Raman spectra. Elemental analyses were performed by Mikroanalytische Laboratorien, Elbach, West Germany.

X-ray Diffraction. X-ray powder diffraction patterns of the samples sealed in 0.5 mm o.d. quartz capillaries were obtained by using a Philips camera (diameter 11.46 cm) with Ni-filtered Cu Kα radiation. Crystals suitable for structure determination were either selected in the drybox under a microscope and sealed inside 0.5 mm o.d. quartz capillaries or transferred in the drybox into a glass apparatus to which 0.5 mm o.d. quartz capillaries were attached. Crystals were then selected and dropped into the capillaries in vacuo. X-ray diffraction was carried out on an Enraf-Nonius CAD4 automated diffractometer. Cell dimensions were obtained by a least-squares refinement of the setting angles of the 25 reflections with θ between 8 and 12°. Intensities were corrected for Lorentz–polarization effects. The structures were solved by the heavy-atom method and refined by full-matrix least squares (F). All atoms were refined anisotropically. DIFABS[28] was used to correct intensities for absorption. In $[ClO_2]^+[RuF_6]^-$, the Ru and the Cl atoms lie on diad axes, while in $[ClF_2]^+[RuF_6]^-$, the two distinct Cl atoms lie on diad axes. All calculations were performed on a Micro Vax II computer using the Enraf-Nonius structure determination package.[29] Analytical scattering factors[30] for neutral atoms were corrected for both $\Delta f'$ and $\Delta f''$ components of anomalous dispersion. Other experimental details appear with the crystal data in Table II or in the supplementary material, while positional parameters are given in Table III.

Materials. Ruthenium pentafluoride, ruthenium tetraoxide, and chloryl fluoride were prepared as described in the literature.[31-34] Commercial fluorine (from Union Carbide), ruthenium powder, and ruthenium dioxide hydrate (both from Merck) were used as received. Commercial HF (from Union Carbide) was dehydrated over bismuth pentafluoride before use.[35] Chlorine trifluoride (from Comurhex) was purified by trap-to-trap distillation, and sodium chlorate (from PUK Co.) was dried in an oven before use.

Table III. Positional Parameters and Their Estimated Standard Deviations

atom	*x*	*y*	*z*	B, Å^2[a]
		$[ClO_2]^+[RuF_6]^-$		
Ru	−0.250	0.0118 (4)	0.250	1.95 (3)
Cl	−0.250	0.380 (1)	−0.250	2.4 (1)
F(1)	−0.257 (1)	0.011 (2)	0.507 (1)	4.0 (2)
F(2)	−0.430 (2)	0.237 (2)	0.242 (2)	4.1 (3)
F(3)	−0.426 (1)	−0.224 (2)	0.242 (1)	3.7 (2)
O	−0.249 (2)	0.507 (3)	−0.088 (2)	4.5 (3)
		$[ClF_2]^+[RuF_6]^-$		
Ru	0.12442 (3)	0.1162 (1)	0.02602 (5)	1.974 (8)
Cl(1)	0.500	0.4160 (5)	0.75	2.25 (4)
Cl(2)	0.250	0.500	0.2412 (3)	2.26 (4)
F(1)	0.5700 (3)	0.111 (1)	0.5366 (6)	4.5 (1)
F(2)	0.4283 (3)	0.349 (1)	0.4579 (5)	4.0 (1)
F(3)	0.3196 (3)	0.355 (1)	0.5917 (5)	4.1 (1)
F(4)	0.6766 (3)	0.109 (1)	0.3984 (6)	4.8 (1)
F(5)	0.4274 (3)	0.134 (1)	0.6743 (4)	3.2 (1)
F(6)	0.3241 (3)	0.109 (1)	0.3840 (5)	4.1 (1)
F(7)	0.7006 (3)	0.389 (1)	0.6603 (5)	4.5 (1)
F(8)	0.5509 (3)	0.399 (1)	0.3040 (5)	3.8 (1)

[a] Anisotropically refined atoms are given in the form of the isotropic equivalent displacement parameter defined as $^4/_3\sum_i\sum_j\beta_{ij}\vec{a}_i\vec{a}_j$.

Synthesis of $[ClO_2]^+[RuF_6]^-$. (a) From ClO_2F and RuF_5. About 0.3 mL of thoroughly dried HF and 2.9 mmol of ClO_2F were condensed onto 0.0862 g (0.440 mmol) of RuF_5 at −196 °C. The red to deep violet mixture was allowed to warm to room temperature very slowly. Yellow-green crystals started precipitating out of the slurry within minutes. The product was first dried overnight in vacuo at −78 °C and then for an additional 2 h at room temperature. A 0.124-g (0.439-mmol) quantity of crystalline material was thus isolated and found to be only sparingly soluble in anhydrous HF. Anal. Calcd: Cl, 12.55; F, 40.35; Ru, 35.78. Found: Cl, 12.31; F, 40.21; Ru, 36.05.

(b) From ClF_3 and RuO_4. A 0.313-g (1.897-mmol) sample of RuO_4 previously dehydrated over P_2O_5 was condensed into a sapphire tube together with 0.813 g (8.856 mmol) of ClF_3 and 2.068 g of HF. The mixture was warmed to room temperature and stirred for 2 days, during which time the solution, initially orange-yellow, turned yellow and a green-yellow solid also started to form. The Raman spectrum of the solution showed that all of the RuO_4 had reacted and that ClO_2F had been formed. The reaction did not yield a detectable amount of volatiles at −196 °C (e.g. O_2, F_2). After evacuation of the volatiles at −78 °C followed by further in vacuo drying at room temperature for a few hours, 0.535 g of a green-yellow solid remained in the sapphire tube. The X-ray powder pattern (see Table I) and the vibrational spectra of this solid were identical with those of $[ClO_2]^+[RuF_6]^-$ prepared by route a above.

Preparation of $[ClF_2]^+[RuF_6]^-$. In a typical reaction, 1.059 g (11.45 mmol) of purified ClF_3 was condensed onto 0.164 g (0.836 mmol) of RuF_5 at −196 °C. The mixture was carefully allowed to warm to room temperature. Within approximately 15 min, all of the RuF_5 had dissolved and a yellow-green, clear solution resulted. Excess ClF_3 was removed in vacuo at −78 °C over a 2-day period, leaving light yellow crystals. These were dried in vacuo at room temperature for an additional 2 h. The product (0.234 g, 0.811 mmol) was found to be virtually insoluble in anhydrous HF and decomposed in the range 110–120 °C. Anal. Calcd: Cl, 12.29; F, 52.68; Ru, 35.03. Found: Cl, 12.46; F, 52.53; Ru, 34.85. The X-ray powder pattern of this salt is given in Table I.

Results and Discussion

Syntheses. The direct synthesis of the salt $[ClO_2]^+[RuF_6]^-$ involves a fluoride ion transfer from chloryl fluoride to ruthenium pentafluoride. As far as the reaction of ClF_3 with RuO_4 to yield

(26) Mallouk, T. E.; Rosenthal, G. L.; Müller, G.; Brusasco, R.; Bartlett, N. *Inorg. Chem.* **1984**, *23*, 3167.
(27) Tobias, K. M.; Jansen, M. *Angew. Chem., Int. Ed. Engl.* **1986**, *25*, 993.
(28) Walker, N.; Stuart, D. *Acta Crystallogr.* **1983**, *A39*, 158.
(29) Frenz, B. A. *SDP Users Guide*; Enraf-Nonius: Delft, The Netherlands, 1983 (version of Jan 6).
(30) *International Tables for X-ray Crystallography*; Kynoch: Birmingham, England, 1974; Vol. IV.
(31) Darriet, J.; Lozano, L.; Tressaud, A. *Solid State Commun.* **1979**, *32*, 493.
(32) Christe, K. O.; Wilson, R. D.; Schack, C. J. *Inorg. Nucl. Chem. Lett.* **1975**, *11*, 161.
(33) McDowell, R. S.; Asprey, L. B.; Hoskins, L. C. *J. Chem. Phys.* **1972**, *56*, 5712.
(34) Sakurai, T.; Takahashi, A. *J. Inorg. Nucl. Chem.* **1979**, *41*, 681.
(35) Christe, K. O.; Wilson, W. W.; Schack, C. J. *J. Fluorine Chem.* **1978**, *11*, 71.

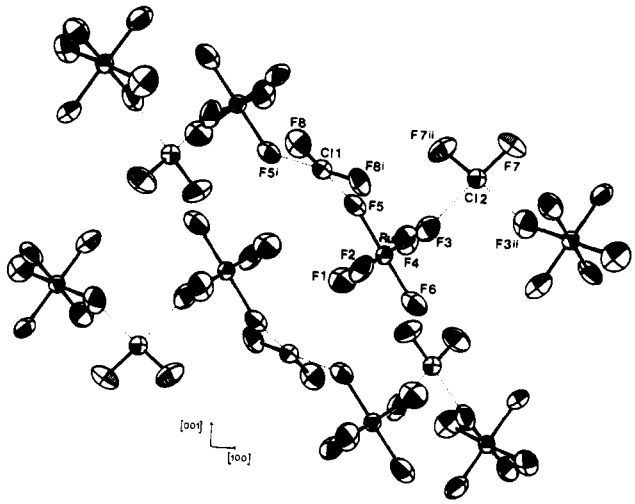

Figure 1. Structure of $[ClF_2]^+[RuF_6]^-$. (In this figure and in Figures 2 and 3, dashed or light solid lines indicate interionic contacts of less than 3 Å.) (i = $-x, y, {}^1/_2 - z$; ii = ${}^1/_2 - x, 1 - y, z$.)

$[ClO_2]^+[RuF_6]^-$ is concerned, thorough drying of RuO_4 prior to use precludes the presence of enough H_2O to form the amount of ClO_2F corresponding to the yield of the salt obtained. Furthermore, H_2O could not arise from the interaction of HF with RuO_4, since there was no sign of a reaction between the two compounds at room temperature during a previous study.[2] On the basis of experimental observations, the following reactions are proposed to explain the formation of the chloryl salt in HF solution:

$$RuO_4 + 2ClF_3 \rightarrow ClO_2F + RuF_5 + ClO_2 \quad (1)$$

$$ClF_3 + 2ClO_2 \rightarrow 2ClO_2F + ClF \quad (2)$$

$$ClO_2F + RuF_5 \rightarrow [ClO_2]^+[RuF_6]^- \quad (3)$$

Reaction 1 was inferred from the observation of both ClO_2F and ClO_2 bands in the Raman spectra of the products of the reaction when it was run with stoichiometric amounts of ClF_3. The detailed mechanism for this reaction is unknown, but all assumptions made should take into account that there was no oxygen evolution observed. The presence of ClO_2 as a product of reaction 1 does not necessarily imply that it arose from the fluorination of a ruthenium-containing species by ClO_2F; it may just as likely be the first-step product from the fluorination of RuO_4 by ClF_3 via, for instance, the intermediate formation of RuO_2F_3. Under these circumstances, ClO_2F could result from the fluorination of this oxide fluoride by ClF_3. Reaction 2[36] accounts for the absence of ClO_2 in the presence of an excess of ClF_3. Probably owing to its weak intensity and its proximity to the Raman band of ClF_3, the band for the ClF molecule could not be observed in the presence of an excess amount of ClF_3. Finally, reaction 3 was demonstrated by the direct synthesis described in the previous section.

Previous preparation of $ClF_3 \cdot RuF_5$ was accomplished by Burns and O'Donnell[6] according to either of the following routes: (i) the reaction of ruthenium metal with an excess of ClF_3 or (ii) the reaction of RuF_6 with excess ClF_3. The former reaction was reported to be extremely violent, while the latter led to mixed products ($[ClF_2]^+[RuF_6]^-$ and $[ClF_4]^+[RuF_6]^-$) that could not be separated. Furthermore, there was some doubt as to whether the product of the reaction involving the bare metal was truly ionic. This will be discussed in some detail later. The reported microanalysis of this species, although reasonable, was however not up to present day standards, with both analyzed elements (Ru and F) yielding slightly lower than calculated values. By first preparing RuF_5 from F_2 and Ru metal at elevated temperature and pressure[31,34] and then distilling onto it purified ClF_3, we were able to prepare the pure salt $[ClF_2]^+[RuF_6]^-$ via a much milder synthetic route. In addition, high-quality crystals were obtainable when care was taken to remove the volatile excess ClF_3 very slowly.

Table IV. Selected Internuclear Distances (Å) and Angles (deg) for $[ClO_2]^+[RuF_6]^-$ and $[ClF_2]^+[RuF_6]^-$

$[ClO_2]^+[RuF_6]^-$ [a]		$[ClF_2]^+[RuF_6]^-$ [b]	
Cl-O	1.379 (9)	Cl(1)-F(8)	1.565 (3)
		Cl(2)-F(7)	1.568 (3)
Cl-F(3)^i	2.494 (8)	Cl(1)-F(5)	2.297 (3)
Cl-F(1)	2.734 (8)	Cl(2)-F(3)	2.263 (4)
Ru-F(1)	1.869 (6)	Ru-F(1)	1.810 (3)
Ru-F(2)	1.814 (8)	Ru-F(2)	1.834 (3)
Ru-F(3)	1.837 (8)	Ru-F(3)	1.885 (4)
		Ru-F(4)	1.828 (4)
		Ru-F(5)	1.886 (3)
		Ru-F(6)	1.825 (3)
O-Cl-O^{iii}	117.2 (9)	F(8)-Cl(1)-F(8)^i	96.4 (3)
		F(7)-Cl(2)-F(7)^{ii}	96.4 (3)
		F(5)-Cl(1)-F(5)^i	92.3 (2)
		F(3)-Cl(2)-F(3)^{ii}	90.9 (2)
F(1)-Ru-F(1)^{ii}	179 (1)	F(1)-Ru-F(2)	91.2 (2)
F(1)-Ru-F(2)	90.2 (4)	F(1)-Ru-F(3)	179.4 (2)
F(1)-Ru-F(2)^{ii}	90.1 (4)	F(1)-Ru-F(4)	90.5 (2)
F(1)-Ru-F(3)	89.9 (3)	F(1)-Ru-F(5)	90.9 (2)
F(1)-Ru-F(3)^{ii}	89.8 (4)	F(1)-Ru-F(6)	91.1 (2)
F(2)-Ru-F(2)^{ii}	91.0 (6)	F(2)-Ru-F(3)	88.4 (2)
F(2)-Ru-F(3)	91.1 (3)	F(2)-Ru-F(4)	177.1 (2)
F(2)-Ru-F(3)^{ii}	177.9 (5)	F(3)-Ru-F(5)	88.7 (2)
F(3)-Ru-F(3)^{ii}	86.8 (4)	F(4)-Ru-F(6)	91.5 (2)
		F(5)-Ru-F(6)	177.9 (2)

[a] i = ${}^1/_2 + x, -y, -{}^1/_2 + z$; ii = $-{}^1/_2 - x, y, {}^1/_2 - z$; iii = $-{}^1/_2 - x, y, -{}^1/_2 - z$. [b] i = $-x, y, {}^1/_2 - z$; ii = ${}^1/_2 - x, 1 - y, z$.

The $[ClF_2]^+[RuF_6]^-$ Structure. A view of the structure showing the atom-numbering scheme is given in Figure 1, while important bond distances and bond angles are listed in Table IV. On first approximation, the structure may be described as consisting of discrete $[ClF_2]^+$ and $[RuF_6]^-$ ions. The cation has the expected C_{2v} symmetry and its Cl-F bond distance of 1.57 Å and F-Cl-F bond angle of 96.4° compare well with the respective values reported for $[ClF_2]^+[SbF_6]^-$[24] and $[ClF_2]^+[AsF_6]^-$,[25] as well as with recent independently calculated[37] theoretical values of 1.58 and 1.60 Å for the bond distance and 100.2 and 98.8° for the bond angle, respectively. In the anion, the ruthenium atom resides in a distorted octahedron of fluorine atoms, with the average Ru-F distance being similar to that found in $[XeF]^+[RuF_6]^-$ and $[XeF_5]^+[RuF_6]^-$.[9]

On closer inspection, interionic contact distances of less than 3 Å between the cation and anion (Cl(1)---F(5) = 2.297 (3) and Cl(2)---F(3) = 2.263 (4) Å) indicate that there is some contribution from a covalently bonded fluorine-bridged arrangement (see also Figure 2). This is further supported by these distances being significantly shorter than those found in $[ClF_2]^+[SbF_6]^-$ (2.33 (3) and 2.43 (3) Å)[24] and $[ClF_2]^+[AsF_6]^-$ (2.34 (1) Å),[25] where a small degree of cation-anion interaction was already postulated. The average ratio of Cl---F to Cl-F distances of 1.455 in $[ClF_2]^+[RuF_6]^-$ is also somewhat smaller than found in the antimony (1.51, average) and arsenic (1.52) salts. However, especially in the former salt, there is a significant uncertainty present in the structural parameters. The more covalent, although still primarily ionic, salt $[BrF_2]^+[SbF_6]^-$ has a more comparable nearest interionic Br---F contact of 2.29 (2) Å, although the ratio of Br---F to Br-F distances has a markedly smaller value of 1.36.[38] Furthermore, two fluorine atoms from each anionic octahedron from cis bridges to $[BrF_2]^+$ to give a helical chain arrangement, which is also the case in the $[ClF_2]^+[RuF_6]^-$ structure. In contrast, $[ClF_2]^+[SbF_6]^-$ and $[ClF_2]^+[AsF_6]^-$ both involve trans fluorine

(36) Bougon, R.; Carles, M.; Aubert, J. *C. R. Acad. Sci. Paris* **1967**, *265*, 179.

(37) (a) Pershin, V. L.; Boldyrev, A. I. *THEOCHEM* **1987**, *150*, 171. (b) Bader, R. F. W.; Gillespie, R. J.; MacDougall, P. J. In *A Physical Basis for the VSEPR Model: The Laplacian of the Charge Density in Molecular Structure and Energetics*; Liebman, J. F., Greenberg, A., Eds.; VCH Publishers: New York, 1989; Vol. 11, p 1-51.

(38) Edwards, A. J.; Jones, G. R. *J. Chem. Soc. A* **1969**, 1467.

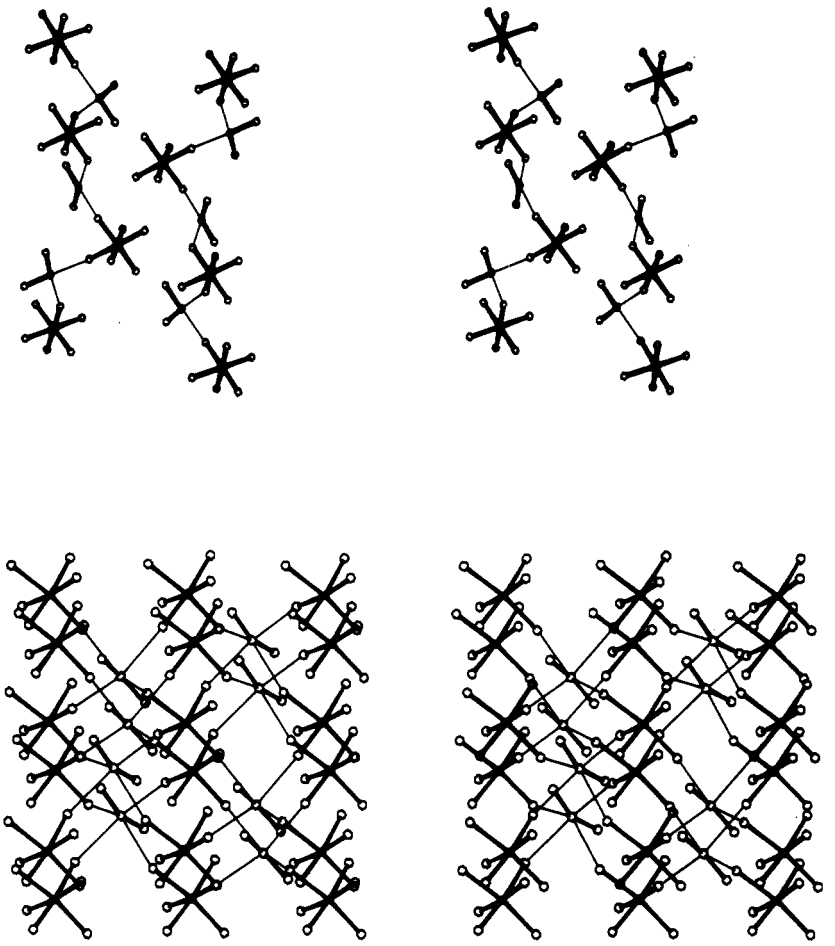

Figure 2. Stereoscopic views of the crystal packings of $[ClO_2]^+[RuF_6]^-$ (top) and $[ClF_2]^+[RuF_6]^-$ (bottom).

bridges between the metal and the chlorine. The weak interionic covalent contribution is also reflected in the relative Ru–F bond distances. The shortest bond (Ru–F(1) = 1.810 (3) Å) is trans to one of the two longest bonds (Ru–F(3) = 1.885 (4) Å), which forms the strongest interionic contact with Cl(2). F(5), involved in the other long bond to Ru, forms the second slightly more distant contact with Cl(1) (there are two crystallographically distinct $[ClF_2]^+$ units in the structure, each with perfect C_{2v} symmetry). The corresponding trans Ru–F(6) bond is only negligibly shorter than the two nonbridging Ru–F bonds, reflecting the weaker contact of F(5) compared to F(3) with the chlorine atoms. The Ru–F(3) and Ru–F(5) bond distances of 1.886 (4) Å are meaningfully longer than the average terminal Ru–F distance of 1.824 Å.

The structure can then best be described as consisting of a helical chain of distorted RuF_6 octahedra (O_h symmetry is lowered to C_s) in contact with the cations via cis bridges to form the expected[25] greatly distorted square-planar environment of fluorine atoms around the chlorine atoms. In light of the previous literature,[24,25,38] it would appear that cis bridging between anion and cation is indicative of significant interionic covalency being present in the structure.

The $[ClO_2]^+[RuF_6]^-$ Structure. The structure of this salt may on first approximation also be described as consisting of discrete cationic and anionic units. A view showing the atom-numbering scheme is given in Figure 3, while important bond distances and bond angles are listed in Table IV. Here, the cation also has the expected C_{2v} symmetry, but both its Cl–O bond distance of 1.379 (9) Å and O–Cl–O bond angle of 117.2 (9)° are slightly smaller than found in other salts containing this cation.[14,20,26,27] The respective values of 1.42 Å and 118.8° predicted for $[ClO_2]^+$ from theory[23] are also slightly greater. For comparison, these values were reported to be 1.475 (3) Å and 117.7 (1.7)° for ClO_2 in the gaseous state.[27] The $[RuF_6]^-$ ion here also exists with the Ru atom in a slightly distorted octahedron of fluorine atoms, with the

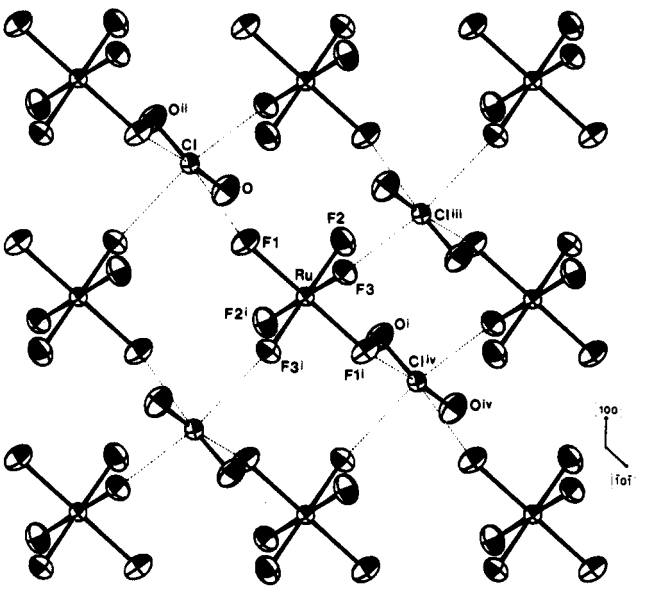

Figure 3. Structure of $[ClO_2]^+[RuF_6]^-$. (i = $1-x, y, {}^1/_2-z$; ii = $-x, y, {}^1/_2-z$; iii = $1-x, -y, 1-z$; iv = $1+x, y, z$.)

average Ru–F bond distance of 1.84 Å being virtually identical with that found in $[ClF_2]^+[RuF_6]^-$.

The primary difference between this structure and that of $[ClF_2]^+[RuF_6]^-$ is that here each Cl atom makes sub 3 Å contacts with four fluorine atoms, all belonging to different $[RuF_6]^-$ units, as shown in Figure 2. Although all four interionic interactions are weaker than those found in the preceding structure, they nevertheless create a two-dimensional array of $[RuF_6]^-$ octahedra with identical orientations, linked along one axis to the $[ClO_2]^+$ units by cis bridges and along another nearly normal axis by trans

Table V. Vibrational Data for $[ClF_2]^+[RuF_6]^-$ and $[ClO_2]^+[RuF_6]^-$

$[ClF_2]^+[RuF_6]^-$ this work		$[ClF_2]^+[RuF_6]^-$ ref 6		$[ClO_2]^+[RuF_6]^-$ this work		
R: $\Delta\nu$, cm^{-1} [b]	IR: ν, cm^{-1} [c]	R: $\Delta\nu$, cm^{-1} [b]	IR: ν, cm^{-1} [c]	R: $\Delta\nu$, cm^{-1} [b]	IR: ν, cm^{-1} [c]	approx assgn[a]
				1300 (0.7)	1300 w 1285 w	$\nu_3(B_1)$, ClO_2^+
	1190 w, b		1228 w, b			comb./over.?
				1058 (3.8)	1060 w	$\nu_1(A_1)$, ClO_2^+
802 (2.1)	790 m, sh	807 (1.4)	808 m, sh			$\nu_3(B_1)$, ClF_2^+
785 (6.9)		791 (4.7)				$\nu_1(A_1)$, ClF_2^+
	770 m, sh	787 (4.4)	787 s			
710 (0.7)		718 (0.4)				$Ru_2F_{11}^-$??
681 (10.0)	680 s, vb, sh	684 (10.0)	690 m, sh			ν_1, RuF_6^-
661 (0.6)				663 (10.0)		
628 (4.0)	620 s, b	631 (3.4)	635 s	620 (3.5)	635 s, b	ν_3, RuF_6^-
				570 (2.8)		
553 (2.8)	545 s	554 (2.7)	555 w, b	551 (4.2)	549 w, sh	ν_2, RuF_6^-
534 (1.5)		535 (1.1)				
522 (1.3)		520 (0.8)				
				518 (1.0)	518 w, sh	$\nu_2(A_1)$, ClO_2^+
	470 m, b				460 w, b	ν_4, RuF_6^-
383 (0.7)	375 m	384 (0.4)				$\nu_2(A_1)$, ClF_2^+
271 (3.4)		277 (3.1)				ν_5, RuF_6^-
268 (4.2)		272 (3.8)		266 (6.7)		
182 (0.3)				220 (0.8)		ν_6, RuF_6^-, or lattice mode

[a] References 3, 6, 12, and 39 were consulted for some of the assignments; comb. = combination, over. = overtone. [b] Uncorrected Raman intensities based on relative peak heights are given in parentheses. [c] w = weak, m = medium, s = strong, v = very, b = broad, sh = shoulder; IR data for this work not optimal—bands very broad and ill-resolved.

bridges. This leads to a grossly distorted octahedral environment around the Cl atoms. The bridging distances however are not equal. The nearest interionic contact is F(3)---Cl and occurs along the "cis-bridging" axis at the face of the triangle defined by the two oxygen atoms and one chlorine atom. At 2.494 (8) Å, this is the shortest (by ≥0.04 Å) interionic contact yet reported for any $[ClO_2]^+$ salt[14,20,26,27] and hence suggests a slightly increased degree of covalency. The contact in the plane of the ClO_2 triangle ("trans-bridging") is 0.24 Å longer and is comparable to that found in other $[ClO_2]^+$ salts. In contrast and for reasons to be discussed later, the nearest Cl---F contacts in $[ClF_2]^+[RuF_6]^-$ and the Sb[24] and As[25] analogues occur approximately parallel to the plane formed by $[ClF_2]^+$; the perpendicular contacts are all >3 Å in length and hence do not play a significant role in these structures. Consistent with the relative bridging distances discussed above is the degree of distortion found in the $[RuF_6]^-$ octahedron. The longest bonds are Ru–F(1) and Ru–F(1)^i, which form the weaker trans bridge to $[ClO_2]^+$. The shortest bonds, Ru–F(2) and Ru–F(2)^i, are trans to Ru–F(3)^i and Ru–F(3), respectively, the latter two forming the nearest contacts with $[ClO_2]^+$. The Ru–F(3) bond distance lies halfway between that of the other two distinct Ru–F bonds, which is not entirely expected since, on the basis of the relative strength of the interionic interactions, this bond would be predicted to be the weakest. Nevertheless, the average bond distance of the "bridging" Ru–F bonds (1.86 Å) is meaningfully longer than that of the "terminal" Ru–F bonds (1.81 Å), as expected. The higher overall structural symmetry found here compared to that present for $[ClF_2]^+[RuF_6]^-$ is also reflected in the site symmetry of the Ru centers, with the respective point groups being C_2 and C_1.

It appears that both $[ClO_2]^+[RuF_6]^-$ and $[ClF_2]^+[RuF_6]^-$ involve a slightly higher degree of interionic interaction than any of the other known structurally analyzed salts containing these cations. However, the ionic structure still very much dominates, especially in the former salt. The presence of a transition metal may in part be responsible for this trend.

Vibrational Studies. $[ClF_2]^+[RuF_6]^-$. The Raman and IR vibrational frequencies as well as their approximate relative intensities and assignments are listed in Table V, together with frequencies obtained previously by Burns and O'Donnell.[6] As expected for a predominantly ionic salt, the band positions are characteristic of distinct $[ClF_2]^+$[39] and $[RuF_6]^-$[3,6] moieties. After

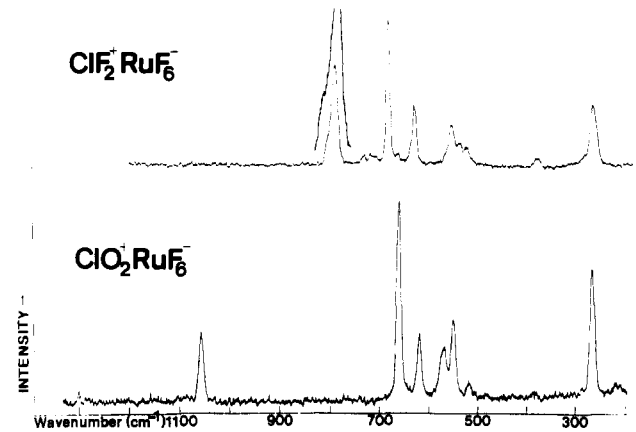

Figure 4. Raman spectra of $[ClF_2]^+[RuF_6]^-$ and $[ClO_2]^+[RuF_6]^-$.

accounting for the bands due to $[ClF_2]^+$ (C_{2v}) (Raman 802, 785, and 383 cm^{-1}; IR 790, 770, and 375 cm^{-1}), we note that the number of bands remaining and their proliferation (especially in the Raman spectrum, which is shown in Figure 4) as well as the apparent lifting of the mutual exclusion rule between Raman- and IR-active modes are all indicative of the symmetry of the $[RuF_6]^-$ moiety being lowered from octahedral. This is consistent with the crystal structure of the salt, as was discussed earlier. Accordingly, the normally (O_h) Raman-inactive ν_3 mode (F_{1u}) is now found at 628 cm^{-1} in the Raman spectrum and the triply degenerate ν_5 mode (F_{2g}) is split into two resolvable bands at 271 and 268 cm^{-1}. The bands present at ~680 cm^{-1} (ν_1, A_{1g}) and 545 cm^{-1} (ν_2, E_g) in the IR spectrum can also only be explained by such a lowering in symmetry, which renders them IR active.

Two features of the Raman spectrum still need explaining: (i) the presence of three bands at 522, 534, and 553 cm^{-1}, which is the region of the ν_2 mode[3,6] (E_g in an octahedral ligand field), and (ii) the presence of two bands (681 and 661 cm^{-1}) in the region of ν_1 (A_{1g} in an octahedral ligand field). Both of these features can be explained as factor group splittings. From the crystal structure, the O_h symmetry of $[RuF_6]^-$ is lowered to a C_1 site symmetry and the factor group (also referred to as space group or crystal group)[40] symmetry is D_{2h}. By referring to relevant

(39) Gillespie, R. J.; Morton, M. J. *Inorg. Chem.* **1970**, *9*, 616.

(40) Fateley, W. H.; McDevitt, N. T.; Bentley, F. *J. Appl. Spectrosc.* **1971**, *25*, 155.

Table VI. Comparison of ν_1 Vibrational Frequencies for $[RuF_6]^-$ with Ru–F Bond Distances in Known Structures

salt	ref	no. of Ru–F(br)[a]	av Ru–F(br) dist, Å[b]	no. of Ru–F(t)[c]	av Ru–F(t) dist, Å[d]	shortest Ru–F, Å	ν_1, Raman $\Delta\nu$, cm^{-1}
$[ClF_2]^+[RuF_6]^-$	this work	2	1.89	4	1.82	1.81	681
$[ClO_2]^+[RuF_6]^-$	this work	4	1.86	2	1.81	1.81	663
$[XeF]^+[RuF_6]^-$	9	1	1.92	5	1.80	1.78	683
$[XeF_5]^+[RuF_6]^-$	9	4	1.86	2	1.82	1.82	n.a.[e]

[a] br = bridging. [b] Average bond distance of Ru–F involved in interionic contacts. [c] t = terminal. [d] Average bond distance of terminal Ru–F bonds. [e] n.a. = not available but ν_1 predicted at ~660 cm^{-1}—see Results and Discussion.

correlation tables,[41] one easily deduces that the ν_2 mode can split into four Raman-active components (A_g, B_{1g}, B_{2g}, and B_{3g}) in this type of symmetry environment. Three of these bands are resolved here, while O'Donnell reports all four.[6] The ν_1 band is split into two bands, both of which appear to be present with greatly varying intensity. The absence of the multitude of expected bands resulting from the factor group splitting of the other modes may be due to accidental overlap and/or inadequate resolution.

The splitting of the ν_1 (A_1) $[ClF_2]^+$ stretching mode reported by O'Donnell and Burns (see Table V)[6] is not observed here. It may in fact be due to instrumental noise or to factor group splitting, which we were not able to resolve. The point symmetry of free $[ClF_2]^+$ (C_{2v}) is reduced slightly to a C_2 site symmetry, with the factor group symmetry of the entire structure being D_{2h}. This results in the ν_1 (A_1) mode being split into two Raman-active modes (A_{1g} and B_{1g}) and one IR-active mode (B_{1u}), which is exactly what was observed in their spectra. The expected splitting of the ν_2 and ν_3 modes is probably not observed for reasons stated above.

The factor group splitting of both the $[RuF_6]^-$ and $[ClF_2]^+$ vibrational modes also explains why some of the resulting band components have significantly different positions in the Raman than in the IR spectra. The site symmetry alone would predict the same frequency for a given band in both cases. The factor group splitting however restores the mutual exclusion rule, thus effecting the observed differences.

Two other spectral features should be mentioned: (i) the very weak band at 710 cm^{-1} in the Raman spectrum and (ii) the comparatively[10,13,39] low frequency of the two $[ClF_2]^+$ stretching modes, ν_1 and ν_3. The band at 710 cm^{-1} was tentatively assigned by Burns and O'Donnell[6] to $[Ru_2F_{11}]^-$, on the basis of the Raman spectrum[3] of $[XeF]^+[Ru_2F_{11}]^-$, and this does appear to be the most feasible explanation. The very minor formation of this species may be due to the onset of sample decomposition in the laser source. The second feature stated above is somewhat more significant. The ν_1 and ν_3 $[ClF_2]^+$ Raman bands of $[ClF_2]^+[SbF_6]^-$ and $[ClF_2]^+[AsF_6]^-$ are found at ~810 and ~820–830 cm^{-1}, respectively.[10] This is 20–30 cm^{-1} higher than their position in $[ClF_2]^+[RuF_6]^-$, which is consistent with the higher degree of interionic covalency (and hence weakening of Cl–F bonds) present in this salt. Interestingly, these bands are found at much more comparable frequencies of 788 and 799 cm^{-1}, respectively, in the Raman spectrum of $[ClF_2]^+[PtF_6]^-$,[15] suggesting that this salt may contain a similar degree of covalency. This further supports the earlier stated postulate that transition-metal centers may play a greater indirect role in the exact nature of the interionic interaction involved in these salts. This will be briefly elaborated upon later in the discussion.

$[ClO_2]^+[RuF_6]^-$. The Raman and IR spectra of this salt are both somewhat simpler than those of their $[ClF_2]^+$ analogue. This is expected from the crystal structure, which shows a lower degree of interionic interaction while involving a higher degree of symmetry. The spectral data are listed in Table V, while the Raman spectrum is shown in Figure 4.

The spectral bands fall in the regions expected for the two ionic moieties $[ClO_2]^+$ [12,13,15,17,18,42] and $[RuF_6]^-$.[3,6] Lower than octahedral symmetry is nevertheless again evident for $[RuF_6]^-$ from the presence of its ν_3 band (F_{1u}) in the Raman spectrum, indicating a relaxation of the mutual exclusion rule. Similarly, the broadness of this band in the IR spectrum suggests that it may be partially overlapping with the ν_1 mode (A_{1g}). Furthermore, the splitting of the ν_2 mode (E_g) in the Raman spectrum is indicative of its double degeneracy being lifted. The C_2 site symmetry of $[RuF_6]^-$ is consistent with these observations. The difference in frequency of the ν_3 band in the IR compared to the Raman spectrum (15 cm^{-1}) may be explained by considering factor group splitting, as discussed earlier. Here, the C_2 site symmetry of $[RuF_6]^-$ is coexistent with C_{2h} factor group symmetry, leading to two mutually exclusive components for this mode.

Three bands are observed in each spectrum for $[ClO_2]^+$ (C_{2v}), as expected. In the IR spectrum, the high-frequency ν_3 band is split into two components. Factor group splitting considerations *cannot* explain this multiplicity because only one IR- and one Raman-active component would result for this mode upon applying such a treatment. Isotope splitting (^{35}Cl and ^{37}Cl) hence appears to be the best explanation, especially since the relative intensity and positions of the two bands are in agreement with theory. Furthermore, the nearly identical split of 14 cm^{-1} that was observed[12] for this fundamental in the IR spectra of $[ClO_2]^+[AsF_6]^-$ and $[ClO_2]^+[BF_4]^-$ was attributed to this effect. Although isotope splitting was also observed in these two salts' IR spectra for the ν_1 and ν_2 bands of $[ClO_2]^+$, inadequate spectral resolution prevented the observation of this effect here for the respective fundamentals of $[ClO_2]^+[RuF_6]^-$. Detailed comparison with other $[ClO_2]^+$ salts of the effect of interionic interaction on the vibrational spectra is not possible, since, to the best of our knowledge, there are no crystal structure reports available for salts of the type $[ClO_2]^+[MF_6]^-$.

Aside from the symmetry effects, there are two other noticeable differences between the $[RuF_6]^-$ bands found in the Raman spectrum here and for $[ClF_2]^+[RuF_6]^-$: (i) the 18-cm^{-1} "red shift" of the most intense band, ν_1,[43] upon substituting $[ClF_2]^+$ with $[ClO_2]^+$ and (ii) the 17-cm^{-1} "blue shift" of the highest frequency ν_2 component upon making the same substitution. The first point above is the more interesting and is most easily explained by first listing the ν_1 frequencies found in the Raman spectra of all previously reported $[Cat]^+[RuF_6]^-$ salts, in increasing order: $[Xe_2F_3]^+[RuF_6]^-$, 652 cm^{-1};[3] $Cs^+[RuF_6]^-$, 656 cm^{-1};[3] $O_2^+[RuF_6]^-$, 660 cm^{-1};[5] $[NO]^+[RuF_6]^-$, 660 cm^{-1};[8] $[ClO_2]^+[RuF_6]^-$, 663 cm^{-1}; $[ClF_2]^+[RuF_6]^-$, 681 cm^{-1}; $[XeF]^+[RuF_6]^-$, 683 cm^{-1}.[3] The striking feature of this progressive series is that the frequency of the band appears to increase with the degree of interionic covalency of each species. A high degree of ionicity in $[Xe_2F_3]^+[RuF_6]^-$ is suspected from the absence of splitting of its ν_2 mode (E_g), which is split in the spectra of all the other salts listed except $Cs^+[RuF_6]^-$. The relatively high degree of interionic bridging present in $[XeF]^+[RuF_6]^-$ is evident from its crystal structure,[9] which features a strong contact between Xe and one of the $[RuF_6]^-$ fluorine atoms (the Xe---F to Xe–F bond distance ratio is only 1.17). The salts $O_2^+[RuF_6]^-$ and $[NO]^+[RuF_6]^-$ are reasonably expected to

(41) Wilson, E. B., Jr.; Decius, J. C.; Cross, P. C. *Molecular Vibrations. The Theory of Infrared and Raman Vibrational Spectra*; McGraw-Hill Book Co., Inc.: New York, 1955.

(42) Carter, H. A.; Johnson, W. M.; Aubke, F. *Can. J. Chem.* **1969**, *47*, 4619.

(43) As is evident from Table V, the ν_1 band of $[RuF_6]^-$ for $[ClF_2]^+[RuF_6]^-$ is split into a very intense high-frequency component and a second much weaker one at lower frequency due to crystal field splitting effects, which reduce the O_h symmetry of the $[RuF_6]^-$ anion. The following paragraph concentrates solely on the much more prominent high-frequency component for the sake of clarity. It must be understood that the ensuing discussion may consequently be oversimplified.

structurally resemble $Cs^+[RuF_6]^-$ more closely than $[XeF]^+[RuF_6]^-$. As expected, the stronger the nonetheless weak interionic contact in these salts is, the more distorted becomes the $[RuF_6]^-$ symmetry from octahedral. This is evident from the two crystal structures presented here and from the other two known $[RuF_6]^-$-containing structures.[9] It then appears that a lowering in point symmetry from O_h at the Ru centers is responsible for an increase in the ν_1 frequency. It also seems that there is a distinct "jump" in the wavenumber from ~660 to ~680 cm^{-1}, coinciding with the advent of significant covalency. To understand why the ν_1 frequency increases in this manner, it is necessary to look at the Ru–F bond types and their respective distances. These are presented in a hopefully meaningful fashion in Table VI, along with the respective ν_1 frequencies. It appears that the position of ν_1 is governed by the average bond length of the "common majority". In other words, if four or five fluorine atoms are in weak contact with the cation, ν_1 occurs at the ~660-cm^{-1} position; the presence of four or five terminal Ru–F bonds places it at ~680 cm^{-1}. Since the ν_1 band in the fully ionic $Cs^+[RuF_6]^-$ is found at 656 cm^{-1}, it would appear that a predominant effect of significant interionic covalency is the strengthening of all or some of the remaining terminal bonds through very weak π backbonding (reduction of electron density around the Ru center) which, when forming a majority, blue-shift the ν_1 frequency from that found in the Cs^+ salt. This explanation is not contradictory to the relative lengths of the shortest Ru–F (terminal) bond(s) in the four known structures and is supported by the following observations: (i) the frequency of the Raman-active mode ν_1 of RuF_6 was calculated[44] to be 675 cm^{-1}, which is in line with the decrease in electron density from that of fully ionic $[RuF_6]^-$; (ii) the tetrameric covalently bridged RuF_5 has one terminal Ru–F bond with a somewhat short length of 1.74 Å[45] (correlating this observation with the vibrational spectra of RuF_5 is beyond the scope of the present paper); and (iii) the most intense Raman band of the singly fluorine-bridged dimer $[Ru_2F_{11}]^-$ in $[XeF]^+[Ru_2F_{11}]^-$ occurs[3] at 716 cm^{-1}, indicating a ~60-cm^{-1} blue shift of what is equivalent to a ν_1 band in $[RuF_6]^-$.[46] The second shifted Raman band mentioned at the beginning of this paragraph does not follow any similar trends, and the shift is therefore attributed to lattice packing effects, which may in fact also partially be responsible for the shift discussed in detail above.

Raman Spectra of $[ClF_2]^+[RuF_6]^-$ and RuO_4 in ClF_3/HF Solution. A Raman spectrum of $[ClF_2]^+[RuF_6]^-$ in anhydrous HF could not be obtained because the salt was surprisingly found to be virtually insoluble in this solvent at room temperature. This was verified by the Raman spectrum of the liquid phase of the two-phase mixture, which did not show any sign of vibrational bands attributable to the salt. Upon addition of ClF_3 to the mixture, a homogeneous solution instantly formed, as was expected in light of the high solubility observed for the salt in ClF_3 alone. The Raman data for this solution are listed in Table VII, along with the data for RuO_4 in ClF_3/HF and the data for the "background" ClF_3/HF solution. The most striking feature of the spectrum is the presence of two partially overlapping bands of nearly equal intensity at 657 and 680 cm^{-1}. The total absence of these bands in the background spectrum and the agreement of their positions with those of the most intense bands present in the Raman spectra of $[ClO_2]^+[RuF_6]^-$ and $[ClF_2]^+[RuF_6]^-$, respectively, lead to both bands being tentatively assigned as the ν_1 mode of $[RuF_6]^-$. However, the presence of only one band (at 657 cm^{-1}) in this region in the Raman spectrum of RuO_4 (or rather $[ClO_2]^+[RuF_6]^-$—see discussion below) in the same solvent medium (see Table VII) makes the presence of the signal at 680 cm^{-1} somewhat puzzling.

Table VII. Raman Data for $[ClF_2]^+[RuF_6]^-$ and RuO_4 in ClF_3/HF Solution[a]

$\Delta\nu$, cm^{-1} [b]			
$[ClF_2]^+[RuF_6]^-$/ClF_3/HF	RuO_4/ClF_3/HF	HF/ClF_3	approx assgn[c]
	1268 w		ν_5, ClO_2F
	1098 s		ν_1, ClO_2F
1053 (<0.1)[d]	1055 s		ν_1, ClO_2^+
782 (0.6)			ν_1, ClF_2^+
763 (0.7)	763 m	763 s	ν_1, ClF_3
680 (0.4)			ν_1, RuF_6^-
657 (0.5)	657 vs		
515 (1.0)	516 vs	516 vs	ν_2, ClF_3
423 (0.1)		425 w	ν_5, ClF_3
	400 m		ν_4, ClO_2F
	361 w		ν_6, ClO_2F
315 (0.1)	315 w	314 m	ν_3, ClF_3
260 (0.3)	260 m		ν_5, RuF_6^-

[a] X:ClF_3:HF mole ratios: X = $[ClF_2]^+[RuF_6]^-$, 1:6:60; X = RuO_4, 1:5:50. [b] See Table V for abbreviation definitions. [c] Assignments made according to refs 6, 12, 39, and 49. [d] This band is the consequence of the extremely moisture-sensitive salt picking up trace amounts of H_2O during its manipulation.

Factor group splitting considerations obviously cannot be applied to solution spectra, and all precautions were taken to avoid having any undissolved $[ClF_2]^+[RuF_6]^-$ in the sample beam. The observed solubility of this salt in ClF_3 but not in HF may be relevant here, and the following equilibria may explain the presence of the high frequency band:

$$[ClF_2]^+[RuF_6]^-(solid) \xrightarrow{ClF_3/HF} [ClF_2]^+(solv) + [RuF_6]^-(solv) \quad (4)$$

$$[ClF_2]^+(solv) + [RuF_6]^-(solv) \rightleftharpoons [ClF_2{\cdot}RuF_6](solv) \quad (5)$$

$$ClF_3 + HF \overset{K_d}{\rightleftharpoons} [ClF_2]^+ + [HF_2]^- \quad (6)$$

Equilibrium 6 has been reported to occur with a dissociation constant of approximately 2×10^{-4}.[47] It is possible that its presence drives the postulated equilibrium (5) to the right, which not only leads to the generation of the solvated[48] species $[ClF_2{\cdot}RuF_6]$ or some similar "molecular" moiety involving interionic contact reminiscent of that present in the solid but also enhances the solubility of the salt. The ν_1 band of "$[RuF_6]^-$" for such a species would be expected at a higher frequency than that of the free anion, according to the arguments presented in the previous section. Although two sets of $[ClF_2]^+$ vibrational fundamentals would be expected in the presence of the equilibrium shown in eq 5, only a single ν_1 band is seen in the solution's Raman spectrum. The absence of ν_2 and ν_3 may be due to accidental overlap with neighboring bands, insufficient intensity, and/or some not easily explainable interaction with the solvent. The second ν_1 ($[ClF_2]^+$) band due to the solvated $[ClF_2{\cdot}RuF_6]$ moiety, which would be expected at a lower frequency than its more ionic counterpart, may be hidden either by the ν_1 band at 782 cm^{-1} or even by the ν_1 fundamental of ClF_3 at 763 cm^{-1}. It is interesting to note that the Raman spectrum[47] of $[ClF_2]^+[SbF_6]^-$ in a ClF_3/HF solution also yields only one band (ν_1) at 785 cm^{-1} due to solvated[48] $[ClF_2]^+$. When this salt is dissolved in HF alone, the position of this band (now resulting from purely ionic[48] $[ClF_2]^+$) is shifted to a significantly higher frequency of 810 cm^{-1}, which interestingly matches its observed frequency in the solid state.[10] These observations, together with the appearance of the ν_1 band of $[ClF_2]^+$ at 785 cm^{-1} for both a dilute solution of ClF_3

(44) (a) Weinstock, B.; Claasen, H. H.; Chernick, C. L. *J. Chem. Phys.* **1963**, *38*, 1470. (b) Weinstock, B.; Goodman, G. L. *Adv. Chem. Phys.* **1965**, *11*, 169.

(45) (a) Holloway, J. H.; Peacock, R. D.; Small, R. W. H. *J. Chem. Soc.* **1964**, 644. (b) Mitchell, S. J.; Holloway, J. H. *J. Chem. Soc. A* **1971**, 2789.

(46) It must be remembered however that, in this compound and in RuF_5, the octahedron around Ru is grossly distorted, and significantly lower than O_h symmetry is present.

(47) Surles, T.; Quaterman, L. A.; Hyman, H. H. *J. Fluorine Chem.* **1973**, *3*, 294.

(48) The distinction between solvation in HF alone ("purely ionic") as depicted in eq 6 and in the combined HF/ClF_3 media (eqs 4 and 5) must be noted.

(49) (a) Surles, T.; Hyman H. H.; Quaterman, L. A.; Popov, A. I. *Inorg. Chem.* **1971**, *11*, 913. (b) Tantot, G. Ph.D. Thesis, Université Pierre et Marie Curie—Paris VI, 1976.

in HF[47] and for solid $[ClF_2]^+[RuF_6]^-$, are consistent with this salt's significant degree of cation–anion interaction, as discussed earlier.

Only one band was observed in the Raman spectrum of the $[ClF_2]^+[SbF_6]^-/ClF_3/HF$ solution in the region of ν_1 for $[SbF_6]^-$,[47] whereas two were observed here in the analogous region for the $[ClF_2]^+[RuF_6]^-$ solution. A noteworthy difference between the two solutions is that whereas an unspecified *excess* of ClF_3 was used in the former study, only 9 mol % ClF_3 in HF was present here. On the basis of data from conductivity and equilibrium studies on ClF_3/HF solutions given in the same paper, the relative concentration of $[ClF_2]^+$ in HF is near maximum between ~5 and 60 mol % ClF_3, dropping off dramatically at higher solute concentrations. Hence, neither the equilibrium nor the resulting solvated "molecular" species described in eq 5 above would be expected to play any similar part in the $[ClF_2]^+[SbF_6]^-$ solution that was utilized[47] for the Raman spectroscopy studies. In contrast, it should be noted that the concentration of solvated $[ClF_2]^+$ in the $[ClF_2]^+[RuF_6]^-$ solution studied here would be increased by ~25% as a consequence of the equilibrium shown in eq 6 above. However, further study of the $[ClF_2]^+[RuF_6]^-$ solution system is needed to validate the above interpretation.

$[ClO_2]^+[RuF_6]^-$ was found to be only sparingly soluble in HF alone, although more so than $[ClF_2]^+[RuF_6]^-$. The apparent extra covalency demonstrated by both salts may be too strong to be balanced by their solvation energy in HF, leading to an enormous reduction in solubility from that of "pure" ionic fluoride salts in this solvent. The relative solubilities of the two salts are consistent with their respective degree of interionic contact.

Finally, it should be noted that some of the expected cationic and anionic bands for both solutions studied are overlapped by the very strong and broad ClF_3 bands. Consequently, more exact assignments of both band intensity and mode were not attempted.

General Discussion. The two crystal structures presented here shine further light on the factors suggested[14,25] to dictate the bonding mechanisms in salts containing the $[ClF_2]^+$ and $[ClO_2]^+$ cations. As found with previous salts studied,[10,14,20,26] $[ClF_2]^+$ forms weak but significantly stronger contacts than $[ClO_2]^+$ with the counteranion. This may be due to the relative spatial position of the nonbonding electrons of the chlorine atoms in each case, as has been suggested previously.[14] In the former case, the cation has a slightly distorted tetrahedral ClF_2E_2 format. This allows relatively close contacts to be made on the FE_2 faces of the tetrahedron, leading to a distorted square-planar ClF_4 moiety. The lone pair of nonbonding electrons in $[ClO_2]^+$ on the other hand is most likely located in the plane of the ClO_2 triangle (exo to it), which effectively screens the cation charge and prevents close contacts along this plane with the counteranion. Consequently, the nearest contacts are found approximately perpendicular to the ClO_2E plane, but they are not as strong as the in-plane ones present in the $[ClF_2]^+$ salt. The unprecedented availability here of the crystal structures of these two cations with a *common anion* allows such and other comparisons to be made.

A striking structural feature not yet mentioned is the large volume (>1000 Å^3) of the $[ClF_2]^+[RuF_6]^-$ unit cell and the presence of eight molecular units per unit cell, which has previously been found for $[ClO_2]^+[GeF_5]^-$, where the anion exists as a cis-bridged polymer.[14] It is somewhat surprising that $[ClF_2]^+[RuF_6]^-$ does not prefer to pack in a simpler arrangement, like its $[ClO_2]^+$ analogue as well as the other known $[ClF_2]^+$- and $[BrF_2]^+$-containing salts.[10] This is a reflection of its somewhat unexpected bonding arrangement, which is discussed below.

It was mentioned earlier that the slightly increased covalency apparent in the structures of $[ClF_2]^+[RuF_6]^-$ and $[ClO_2]^+[RuF_6]^-$ compared to their analogues with different anions may in part be due to the presence of a transition metal and bonding d electrons. During their discussion of the crystal structure of $[ClF_2]^+[AsF_6]^-$, Lynton and Passmore[25] stated that the structures of $[ClF_2]^+$ salts lie somewhere between ionic (molecular orbitals around Cl atoms sp^3 hybridized) and bridging (molecular orbitals around Cl atoms d^2sp^3 hybridized). The predominant former configuration leads to a distorted tetrahedral ClF_2E_2 environment around the chlorine atoms, whereas the latter leads to a distorted octahedral ClF_4E_2 arrangement.[25] Shorter interionic distances and the approach of the F_2–Cl---F_2 environment toward square planarity are two primary indicators of a structure in which the bridging component has increased importance. Whereas the interionic distances for $[ClF_2]^+[RuF_6]^-$ have already been shown to be slightly shorter than usual, increased approach to square planarity of the ClF_4 unit is indicated by the following parameters: (i) the longest F–F distances of 3.23 and 3.31 Å between the two pairs of fluorine atoms (F(3)–F(3)^{ii} and F(5)–F(5)^{i}, respectively) involved in the interionic contacts (see Figure 1) are shorter than those found in any of the other reported $[XF_2]^+[MF_6]^-$ (X = Cl, Br) salts ($[ClF_2]^+[SbF_6]^-$, 3.36 Å;[24] $[ClF_2]^+[AsF_6]^-$, 3.41 Å;[25] $[BrF_2]^+[SbF_6]^-$, 3.39 Å[38]) and, more importantly, (ii) the standard deviations of ±0.37 and ±0.41 Å among the four F–F distances comprising the square planes around the two distinct Cl atoms are both smaller than ±0.42 and ±0.44 Å present for $[ClF_2]^+[SbF_6]^-$ and $[ClF_2]^+[AsF_6]^-$, respectively. As was stated previously, the structure of $[BrF_2]^+[SbF_6]^-$[38] most closely resembles that of $[ClF_2]^+[RuF_6]^-$ and accordingly this parameter has a more comparable value of ±0.39 Å. Although the differences among these values are small, they appear to be meaningful. A ClF_4E_2 environment is present around the chlorine atoms in the ion ClF_4^-, and semiionic three-center–four-electron bonds have been postulated to explain the bonding present.[37a] The apparently greater albeit still secondary contribution from this type of bonding in $[ClF_2]^+[RuF_6]^-$ compared to that present in the Sb[24] and As[25] analogues suggests that the degree of multicentered bonding in these types of ClF_2^+ salts may be slightly enhanced by the presence of bonding d orbitals. Due to the significantly weaker magnitude and greater complexity of the interionic contacts in $[ClO_2]^+[RuF_6]^-$, a complete treatment of this sort cannot be successfully applied. However, multicentered bonding cannot be accommodated here, since each oxygen ligand involves two chlorine valence electrons in bonding and consequently the two chlorine p orbitals required are wholly used in these Cl–O bonds.

Further evidence for the significance of the interionic contacts in $[ClF_2]^+[RuF_6]^-$ comes from its magnetic moment, which with a value of 3.64 μ_B[6] is somewhat lower than the expected spin-only value of 3.88 μ_B and the calculated (Curie constant correction applied) value of 3.83 μ_B[50] (it must however be acknowledged that the analytical data presented for this salt in ref 6 were not optimal). In addition, this value is very similar to that found for the tetrameric RuF_5 (3.60 μ_B) at a similar temperature.[50] More importantly, the magnetic behavior of the latter was later studied in detail at low temperatures and antiferromagnetic coupling was found to occur through the bridging fluorine atoms between the four Ru centers, with a maximum in magnetic susceptibility at 40 K.[31,51] It would consequently be of interest to undertake such a study with $[ClF_2]^+[RuF_6]^-$ (and $[ClO_2]^+[RuF_6]^-$) to check for this behavior and hence to gain further insight into the nature of the interionic covalency. These studies are presently at the planning stage.

In summary, the presence of a transition metal appears to lend a slightly greater degree of covalency to the structures of $[ClF_2]^+[RuF_6]^-$ and $[ClO_2]^+[RuF_6]^-$ than observed previously for their respective analogues with different metals. This effect is more pronounced in the former salt. Both materials are however overall best described as being ionic. The relatively low degree of symmetry in the structure of $[ClF_2]^+[RuF_6]^-$ results in its vibrational spectra having some second-order characteristics, all of which are explainable.

Acknowledgment. The assistance of Jacques Isabey with some of the technical aspects of this work is much appreciated.

Supplementary Material Available: Tables of crystal data, bond distances and bond angles, atomic positional parameters, anisotropic thermal parameters, and lattice constants and space groups (7 pages); tables of calculated and observed structure factors (6 pages). Ordering information is given on any current masthead page.

(50) Holloway, J. H.; Peacock, R. D. *J. Chem. Soc.* **1963**, 527.
(51) Hattori, T.; Idogaki, T.; Uryū, N. *Phys. Status Solidi B* **1988**, *148*, K47.